YMTHE, Volume *27*

Supplemental Information

A Mitochondrial VDAC1-Based Peptide Greatly Suppresses Steatosis and NASH-Associated Pathologies in a Mouse Model

Srinivas Pittala, Yakov Krelin, Yael Kuperman, and Varda Shoshan-Barmatz

Supplementary Materials

A mitochondrial VDAC1-based peptide greatly suppresses steatosis- and NASH-associated pathologies in a mouse model

Srinivas Pittala[1], Yakov Krelin[1], Yael Kuperman[2] and Varda Shoshan-Barmatz[1#]

Materials and Methods

Materials

Bovine serum albumin (BSA), beta-mercaptoethanol,4',6-diamidino-2-phenylindole (DAPI), dithiothreitol (DTT), HEPES, a PLA (proximity ligation assay) kit and periodic acid-Schiff's (PAS) reagent, picric acid, phenylmethylsulfonyl fluoride (PMSF), propidiumiodide, reactive red-agarose, Tris, trisodium citrate, sirius red, sucrose, streptozotocin, Triton X-100, Tween-20 and ethylene glycol-bis(β-aminoethyl ether)-N,N,N',N'-tetraacetic acid (EGTA) were purchased from Sigma (St. Louis, MO). Eosin, glycogen, hematoxylin, oil red O, heparin and were purchased from Fisher Scientific (Geel, Belgium), leupeptin, and a Masson trichrome staining kit were from Bio-optica (Milano, Italy), and a TUNEL staining kit was obtained from Promega (Madison, WI). Dimethyl sulfoxide (DMSO) was purchased from MP Biomedicals (Solon, OH). Power SYBER green master mix was from Applied Biosystems (Carlsbad, CA). Formaldehyde was purchased from Emsdiasum (Hatfield, PA). 3,3-diaminobenzidine (DAB) was obtained from ImmPact-DAB (Burlingame, CA). Primary and secondary antibodies, their sources, and the dilutions used are detailed in Table S2. R-Tf-D-LP4 peptide (KWTWK-216-NSNGATWALNVATELKK-199-EWTWSHRPYIAH), comprising 34 residues in D configuration (except the underlined Tf sequence)[1] was synthesized by GL Biochem (Shanghai, China) to >95% purity. The peptide was first dissolved in DMSO as a 40 mM solution and then diluted 20-fold in the appropriate buffer. Peptide concentrations was determined using absorbance at 280 nm and the specific molar excitation coefficient.

Steatosis-NASH-HCC, STAM mouse model

Male C57Bl/6 mice were purchased from Envigo (Jerusalem, Israel). Steatosis-NASH-HCC model mice were induced by a single, low dose (200 µg/mouse) sub-cutaneous injection of streptazotocin (STZ) in 2 day-old mice. From the end of week 4, the mice were fed the HFD-32 high fat diet[2]. The mice manifested steatosis at 6 weeks and NASH at 8 weeks, which progressed to fibrosis at 10 weeks, and finally developed into HCC, starting at week 12 (Figure 1A)[2]. Mice were treated with R-Tf-D-LP4 (14 mg/kg) from week 6-8 for steatosis and from week 9-12 for NASH. The peptide (in 100 µl of Hank's balanced salts solution (HBSS) without calcium buffer) was intravenously administered three times a week. A control group was intravenously injected with 100 µl of 0.8% DMSO in HBSS buffer.

At the end of the experiment, the mice were anesthetized with ketamine (100 mg/kg) and xylazine (10 mg/kg) in PBS for bleeding to obtain plasma for analysis of liver function markers. The mice were then sacrificed by CO_2 inhalation. Livers were removed, photographed, weighed, part was immediately frozen in liquid nitrogen for immunoblotting and qPCR analysis, while the other part was fixed with formaldehyde, embedded in paraffin, sectioned, and subjected to hematoxylin/eosin (H&E) staining or IHC staining, as described below. For assessing fat content, part of the liver was frozen in O.C.T. (optimal cutting temperature) compound, embedded, sectioned and stained with oil red O. The experimental protocols used were approved by the Institutional Animal Care and Use Committee.

Dietary interventions

HFD-32 [2] (507.6 kcal/100 g, 56.7% kcal from fat) comprises 5% egg white powder (MM Ingredients, Wimborne, UK), 6.928% lactose (Pharma Grade, Nelson, UK), 15.88% beef fat (contains 80% beef fat), 5% AIN93G-mineral mixture, 0.002% tertiary butyl hydroquinone and 1.4% AIN93VX-vitamin mix (MP Biomedical, Illkirch, France), 24.5% milk casein (Shaanxi Fuheng Biotechnology, Xi'an, China), 20% safflower oil (high oleic acid content) (Bustan Briut, Galil, Israel), 6.45% sucrose, 0.43% L-cysteine, 5.5% crystalline cellulose (Sigma), 0.36% choline bitartrate and 8.25% maltodextrin (Bulk Powders, Colchester, UK). Control C57Bl/6 mice were fed with a standard chow diet (408.4 kcal/100g, 57% kcal from carbohydrates, 27% kcal from proteins, 16% from fat (V1154-703, Sniff Spezialdäten, Sosset, Germany).

Biochemical analysis

Serum biochemical liver function markers and fat metabolism status, including albumin, urea, alkaline phosphatase (ALP), aspartate aminotransferase (GOT/AST), alanine aminotransferase (GPT/ALT), cholesterol and triglyceride levels, were measured using standard clinical laboratory services. Blood glucose levels were measured using an Accu-Check Performa blood glucose meter.

Histological analysis

Liver histology was assessed by H&E staining of paraffin-embedded sections using standard commercially available methods. Fibrosis was assessed by both Masson's trichrome and sirius red staining of paraffin-embedded sections using established methodologies[3]. Briefly, liver tissues, fixed and embedded in paraffin sections, were stained with a 0.1% sirius red-picric solution. Sections were washed rapidly with acetic acid and photographed under a light microscope (Leica DM2500).

Immunohistochemistry, immunofluorescence and immunoblotting analysis of liver tissue

Immunohistochemical and immunofluorescent staining were performed on 5 μm-thick formalin-fixed and paraffin-embedded liver tissue sections. Sections were deparaffinized (5 minutes in xylene, 3 times), followed by rehydration with a graded ethanol series (100-50%). Antigen retrieval was performed by 30 min incubation in 0.01 M citrate buffer, pH 6.0 (VDAC1, Glut1, LDH-A, GAPDH, HK-I, HK-II, ATP synthase-5a, CPT1a, α-SMA) and for F4/80, in 10 mM Tris-EDTA, pH 9 at 95-98°C. Sections were washed with PBS, pH 7.4, containing 0.1% Triton-X100, incubated in 10% NGS

for 2 h, followed by overnight incubation at 4°C with primary antibodies (see Table S2). Sections were washed with PBS, 0.1% Tween-20 (PBST). For immunohistochemical staining, endogenous peroxidase activity was blocked by incubating the sections in 3% H_2O_2 for 15 min. Following washing with PBST, sections were incubated for 2 h with the appropriate secondary HRP-conjugated antibodies. Sections were washed with PBST and peroxidase activity was visualized by incubating with DAB. After rinsing in water, the sections were counter-stained with hematoxylin, and mounted with mounting medium. Finally, the sections were observed under a light microscope (Leica DM2500) and images were collected at 20× magnification with the same light intensity and exposure time. Non-specific control experiments were carried out using the same protocols but omitting incubation with primary antibodies. For immunofluorescence, Alexa fluor 488-conjugated anti-rat (1:500) secondary antibodies were used. The cells were then stained with DAPI (0.07 μg/ml) and viewed with an Olympus IX81 confocal microscope.

For immunoblotting, proteins in liver lysates were resolved by SDS–PAGE and electro-transferred to nitrocellulose membranes that were subsequently blocked with 5% non-fat dry milk and 0.1% Tween-20 in TBS, incubated with primary antibodies (sources and dilutions listed in Table S2) and then with horseradish peroxidase (HRP)-conjugated anti-mouse, anti-rabbit (1:10,000) or anti-goat (1:20,000) IgG. Blots were developed using enhanced chemiluminescence (Biological Industries). Band intensities were analyzed by densitometry using FUSION-FX (Vilber Lourmat, France) software and values were normalized to the intensities of the appropriate β-actin signal that served as a loading control.

Fat staining with oil red O

Freshly isolated livers were embedded in OCT (optimal cutting temperature) medium and kept at -80ºC until sectioning using a cryotome. Sections (10 μm) were washed with PBS, fixed with (4% formaldehyde, 10 min), gently washed with 60% isopropanol and stained with a solution of 0.5 g oil red O in 60% isopropanol for 15 min. The stained sections were washed with distilled water several times to remove free dye. Then, the samples were counter-stained with hematoxylin for 5 min and images were collected using a light microscope (Leica DM2500).

TUNEL assay

Fixed liver sections in paraffin were processed for a TUNEL assay using the DeadEnd Fluorometric TUNEL system (Promega, Madison, WI) according to the manufacturer's instructions. Sections were deparaffinized, equilibrated in PBS, permeabilized with proteinase K (20 μg/ml in PBS), post-fixed in 4% paraformaldehyde, and incubated in TdT reaction mix for 1 h at 37°C in the dark. The slides were then washed in saline-sodium citrate (SSC) buffer and counter-stained with PI (1 μg/ml). After mounting with Vectashield mounting medium (Vector Laboratories, Burigame, CA), images were collected using a confocal microscope (Olympus IX81).

Glycogen level measurements

To assess glycogen amounts, frozen liver tissue (50 mg) was treated with 0.3 ml of 30% KOH and maintained for 30 min in a boiling water bath. Glycogen was precipitated by adding 100 ul of 1M Na_2SO_4 and 800 µl of ethanol, thoroughly mixed and gently brought to boil in a water bath. A glycogen-rich pellet was obtained by centrifugation at 10,000 g for 5 minutes. After decanting the supernatant, the pellet was dissolved in 0.2 ml H_2O, followed by a second precipitation with ethanol and Na_2SO_4 and centrifugation. The precipitation was repeated a third time. The precipitate was dissolved in 2 ml distilled water and 4 ml of 0.2% anthrone in 95% sulphuric acid was added under ice-cold conditions, then heated for 10 min in boiling water, cooled immediately and the color was read at 680 nm. The amount of glycogen is expressed as mg/g wet tissue. A standard curve was obtained using glucose (0-200 µg) subjected to anthrone in sulphuric acid treatment, as described above.

Fixed liver sections in paraffin were used for glycogen level determination using periodic acid-Schiff (PAS) staining as described previously[4]. Briefly, deparaffinized liver sections (5 µm) were kept in 0.5% periodic acid, washed in water then treated with Schiff's reagent for 15 min, rinsed and counter-stained with hematoxylin for 1 min. Stained sections were visualized and images were collected using a confocal microscope (Olympus IX81).

RNA preparation, real-time PCR (q-PCR) and proteomics analysis

Total RNA was isolated from liquid nitrogen frozen livers obtained from chow-fed (control) or HFD-32 fed peptide-treated mice using an RNeasy mini kit (Qiagen) according to the manufacturer's instructions. Total RNA quality was analyzed using the Agilent RNA 6000 nano kit. Complementary DNA was synthesized from 1 µg total RNA using a Verso cDNA synthesis kit (Thermo Scientific). q-PCR was performed with specific primers in triplicate, using Power SYBER green master mix. Samples were amplified by a 7300 Real Time PCR System (Applied Biosystems) for 40 cycles using the following PCR parameters: 95°C for 15 seconds, 60°C for 1 minute, and 72°C for 1 minute. The copy numbers for each sample were calculated by the CT-based calibrated standard curve method. Target gene levels were normalized relative to α-actin mRNA, serving as an internal control. The mean fold change (± SEM) of the three replicates was calculated. Genes examined and primers used are listed in Table S3.

CPT1-ACSL1- VDAC1 complex purification

CPT1 was purified from isolated rat liver mitochondria, using column chromatography. Rat liver mitochondria (10 mg/ml) were incubated for 40 min on ice in a solution containing 5 mM Tris, pH 7.5, 40 mM β-octyl glucoside (OG) and 0.2 mM phenylmethanesulfonylfluoride and 0.5 ug/ml leupeptin. After centrifugation (40,000g for 40 min at 4ºC), the pellet was re-suspended in half of the original volume and subjected to a second extraction, as above. The combined extracts were loaded onto a reactive red-agarose column, pre-equilibrated with 20 mM Tris, pH 7.25, 5 mM NaCl containing 15 mM OG, 5% glycerol (Buffer A). The loaded column was washed with buffer A, followed by wash

with buffer A containing 50 mM NaCl, then with 100 mM NaCl. The flow-through and wash with buffer A were found to contain 4 proteins, CPT1, VDAC1, ACSL1 and CPT2. Fractions containing the proteins were pooled and concentrated using an Amicon Ultra 4 (10 kDa) concentrating unit. Next, this concentrated fraction was applied to a Sephacryl S-200 column (HiPrep 16/60 Sephacryl S-200 HR) pre-equilibrated with 20 mM Tris, pH 7.25, 10 mM NaCl containing 10 mM OG. Fractions (1.2 ml each) were collected and immunoblotted for CPT1, VDAC1, ACSL1 and CPT2 using specific antibodies.

Proximity ligation assay (PLA)

VDAC1-CPT1a, VDAC1-ACSL1 and CPT1a-ACSL1 interactions were analyzed using a PLA[5] targeting the CPT1/ACSL1/VDAC1 complex at the OMM. Briefly, formalin-fixed and paraffin-embedded liver sections (5 μm-thick) were deparaffinized and permeabilized using 0.3% Triton X-100 in PBS for 30 min. *In situ* PLA experiments were done according to the manufacturer's protocol (Sigma-Aldrich). Briefly, VDAC1 (rabbit anti-VDAC1 primary antibodies) and CPT1a (mouse anti-CPT1a primary antibodies) or VDAC1 (mouse anti-VDAC1 primary antibodies) and ACSL1 (rabbit anti-ACSL1 primary antibodies) or CPT1a (mouse anti-CPT1a primary antibodies) and ACSL1 (rabbit anti-ACSL1 primary antibodies) were probed. As a control, the assay was performed with VDAC1 (OMM) mouse anti-VDAC1 primary antibodies) and citrate synthase (CS) (rabbit anti-CS primary antibodies) (matrix). The concentrations of the antibodies used were based on conventional indirect immunofluorescence staining of the liver sections. The secondary anti-mouse and anti-rabbit IgG (PLA probe MINUS and PLUS) conjugated to complementary oligonucleotide extensions were added. The oligonucleotides hybridized with the subsequently added connector oligonucleotides, allowing the formation of a circular DNA template. This circular DNA molecule was ligated and amplified, thereby creating a single-stranded DNA product covalently attached to one of the proximity probes, and hybridized Texas red-labeled oligonucleotide probes were detected. Preparations were mounted in Vectashield mounting medium (Vector Laboratories) images were collected using a confocal microscope (Olympus IX81).

Assessing metabolic parameters using metabolic cages

Four week-old mice were HFD-32-fed and at week 8 were individually housed in metabolic cages for 5 days. The mice were acclimatized for 24 h prior to 120 h continuous recording of respiratory exchange ratio (RER), O_2 consumption, CO_2 production, energy expenditure and locomotor activity. Water intake, food intake, and body weight were also measured. Locomotor activity: for automated monitoring of locomotor activity, peptide-treated or -untreated mice in the steatosis state were individually housed in PhenoMaster system metabolic chambers (TSE-Systems, Bad Homburg, Germany) for 5 days before termination of the experiment. Locomotor activity was measured continuously over the 5 days of the experiment, using a comprehensive lab animal monitoring system (Columbus Instruments, Columbus, OH). Indirect calorimetry: whole-body oxygen consumption,

respiratory exchange and metabolic rates were measured by indirect calorimetry using a four-chamber open-circuit Oxymax system (Columbus Instruments) to assess the volume of oxygen consumed (VO_2) and the volume of carbon dioxide produced (VCO_2) at 15 min intervals for 120 h. The metabolic rate (kilocalories per hour) was calculated using the following equation: $(3.815 + 1.232 \times RER) \times VO_2$, where RER is the respiratory exchange ratio (VCO_2/VO_2). To calculate total caloric intake, the following values were used: Chow-408.4 kcal/100g (16% from fat), HFD-32 -507.6 kcal/100g (56.7% kcal from fat).

Table S1, Summary of NAFLD Activity Score (NAS)

The scoring of steatosis, ballooning, inflammation and fibrosis was carried out as previous described[6] on livers section from mice at the steatosis and NASH stages subjected to HFD-32 without or with peptide treatment with liver sections from 10 mice of each group were analyzed. H&E staining was used to evaluate for steatosis, ballooning and inflammation. Sirius red staining was used for scoring hepatic fibrosis. Steatosis was determined by analyzing hepatocellular vesicular steatosis. Inflammation was evaluated by counting the number of inflammatory foci per field. Hepatic fibrosis was evaluated in the sirius red stained sections by scoring whether collagen staining was absent (present only in vessels) or was observed within the liver section, with the latter being further defined as mild, moderate or massive.

Steatosis stage parameters	**HFD-32** (Mean ± SD)	**HFD-32 + R-Tf-D-LP4** (Mean ± SD)
Steatosis	2.8 ± 0.2	1.0 ± 0.1
Lobular inflammation	2.6 ± 0.1	1.1 ± 0.1
Hepatocellular ballooning	1.9 ± 0.2	1.0 ± 0.1
NAS score	**7.3 ± 0.16**	**3.1 ± 0.1** (p-value = 0.0070)
NASH stage parameters	**HFD-32** (Mean ± SD)	**HFD-32 + R-Tf-D-LP4** (Mean ± SD)
Steatosis	1.2 ± 0.2	0.5 ± 0.2
Lobular inflammation	3.0 ± 0.1	1.1 ± 0.1
Hepatocellular ballooning	2.0 ± 0.1	1.2 ± 0.2
Fibrosis stage	3.4 ± 0.2	1.5 ± 0.2
NAS score	**9.6 ± 0.15**	**4.3 ± 0.17** (p-value = 0.0492)

Table S2: Antibodies Used in This Study

Antibodies against the indicated protein, their catalogue number, source and the dilutions used in IHC and immunoblot experiments are listed.

Antibody	Source and Catalog No.	Dilution		
		IHC	WB	IF/PLA
Mouse monoclonal anti-actin	Millipore, Billerica, MA, MAB1501	-	1:40000	-
Rabbit polyclonal anti-acetyl-CoA carboxylase 1 (ACC1)	Cell Signaling Technology, Danvers, MA, CST-4190	-	1:2000	-
Rabbit polyclonal anti-ACSL1	Cell Signaling Technology, Danvers, MA, CST-4047S	-	1:3000	1:200
Rabbit polyclonal anti-alpha smooth muscle actin	Abcam, Cambridge, UK, ab5694	1:200	-	-
Rabbit polyclonal Anti-AMPK alpha 1 (phospho T183), AMPK alpha 2 (phospho T172)	Abcam, Cambridge, UK, ab23875	-	1:5000	-
Mouse monoclonal anti-ATP5a	Abcam, Cambridge, UK, ab14748	1:300	-	-
Rabbit polyclonal anti-citrate synthase	Abcam, Cambridge, UK ab96600	1:200	1:2000	-
Mouse monoclonal anti-CPT1a	Abcam, Cambridge, UK ab128568	1:300	1:4000	-
Mouse monoclonal anti-CPT2	Abcam, Cambridge, UK ab110293	-	1:3000	-
Rat monoclonal anti-F4/80	Santa Cruz Biotechnology, Dallas, TX, sc52664	1:150	-	-
Rabbit monoclonal anti-fatty acid synthase (FAS)	Cell Signaling Technology, Danvers, MA, CST-3180	-	1:3000	-
Mouse monoclonal anti-GAPDH	Abcam, Cambridge, UK, ab9484	1: 200	1:2000	-
Rabbit monoclonal anti-Glut1	Abcam, Cambridge, UK, ab40084	1: 200	-	-
Mouse monoclonal anti-HK-I	Abcam, Cambridge, UK, ab105213	1:300	1:2000	-
Rabbit polyclonal anti-HK II	Abcam, Cambridge, UK, ab3279	1:300	1:2000	-
Goat polyclonal anti-LDH-A	Santa Cruz Biotechnology, Dallas, TX, sc-27230	1:200	1:1000	-
Rabbit polyclonal anti-PPARγ	Abcam, Cambridge, UK, ab45036	-	1:2000	-
Rabbit polyclonal anti-SIRT1	Millipore, Billerica, MA, 07-131	-	1:2000	-
Rabbit polyclonal anti-SIRT6	Abcam, Cambridge, UK, ab124293	-	1:2000	
Mouse monoclonal anti-TGF-β	Santa Cruz Biotechnology, Dallas, TX, sc-52893	-	1:2000	-
Rabbit polyclonal anti-UCP1	Abcam, Cambridge, UK, AB10983	-	1:2000	-
Mouse monoclonal anti-UCP2	Cell Signaling Technology, Danvers, MA, #89326	-	1:2000	-
Rabbit monoclonal anti-VDAC1	Abcam, Cambridge, UK, ab15895	1:500	1:5000	1:500

Mouse monoclonal anti-VDAC1	Millipore, Billerica, MA, MABN504	-	-	1:500
Donkey anti-goat-HRP	Abcam, Cambridge, UK, ab97120	1:500	1:15000	-
Goat anti-mouse-HRP	Abcam, Cambridge, UK, ab97040	1:250	1:10,000	-
Goat anti-rabbit-HRP	KPL, Gaithersburg, MD, 474-1506	1:500	1:15,000	-
Goat anti-rat-HRP	Santa Cruz Biotechnology, Dallas, TX, sc-2006	1:500	-	-
Goat anti-rat Alexa fluor 488	Life Technologies, Carlsbad, CA, A11006	-	-	1:1000

Table S3: Real-Time PCR Primers Used in this Study

The genes examined, and the forward and reverse sequences of the primers used are indicated

Gene	Primer sequences
ß-Actin	Forward 5'-ACTCTTCCAGCCTTCCTTCC-3' Reverse 5'-TGTTGGCGTACAGGTCTTTG-3'
IL1ß	Forward 5'- TGCCACCTTTTGACAGTGATG-3' Reverse 5'-TGATGTGCTGCTGCGAGATT-3'
TNFα	Forward 5'-TAGCCCACGTCGTAGCAAAC-3' Reverse 5'-GCAGCCTTGTCCCTTGAAGA-3'
IL6	Forward 5'-TCTGCAAGAGACTTCCATCCA-3' Reverse 5'-TAAGCCTCCGACTTGTGAAG-3'
TGF- ß	Forward 5'- GAACTCCCAACTACAGGACCT-3' Reverse 5'-AATGACAGTGCGGTTATGGC-3'
ACADL	Forward 5'-AGTGTATCGGTGCCATAGCC-3' Reverse 5'-TGATGAACACCTTGCTTCCA-3'
HADH	Forward 5'-ACCAAACGGAAGACATCCTG-3' Reverse 5'-AGCTCAGGGTCTTCTCCACA-3'
ACSL1	Forward 5'-CCGGATGTTCGACAGAATTT -3' Reverse 5'-ATCCCACAGGCTGTTGTTTC-3'
ACSL5	Forward 5'-GCCTGAAATCCTTTGAGCAG-3' Reverse 5'-GGCAAGCTCTACTCGTTTGG-3'
CPT1a	Forward 5'-GAAGAACATCGTGAGTGGCG-3' Reverse 5'-ACCTTGACCATAGCCATCCA-3'
PPARα	Forward 5'-TGCAGCCTCAGCCAAGTTGAA-3' Reverse 5'-TTCCCGAACTTGACCAGCCA-3'
PGC1a	Forward 5'-TGTGTGCTGTGTGTCAGAGT-3' Reverse 5'-ACCAGAGCAGCACACTCTATG-3'
PPARγ	Forward 5'-GCTCCAAGAATACCAAAGTGCG-3' Reverse 5'-CCTTGCATCCTTCACAAGCA-3'
FXR	Forward 5'-GGGGATGAGCTGTGTGTTG-3' Reverse 5'-CACGGCGTTCTTGGTAATG-3'
ADRP1	Forward 5'- GGAGTGGAAGAGAAGCATCG-3' Reverse 5'-TGGCATGTAGTCTGGAGCTG-3'
UCP1	Forward 5'-GGATGGTGAACCCGACAACT-3' Reverse 5'-CTTGGATCTGAAGGCGGACT-3'
UCP2	Forward 5'-TGCGGTCCGGACACAATAG-3' Reverse 5'-GCCTCCAAGGTCAAGCTTCT-3'
SREBP1A	Forward 5'-GAAGACATGCTCCAGCTCATC-3' Reverse 5'-AGGCCAGAGAAGCAGAAGAGA-3'

SREBP1C	Forward 5'-CTGTCGGGGTAGCGTCTG-3' Reverse 5'-CATAGGGGGCGTCAAACA-3'
FASN	Forward 5'-CCCTTGATGAAGAGGGATCA-3' Reverse 5'-ACTCCACAGGTGGGAACAAG-3'
ACC1	Forward 5'-GCCTCTTCCTGACAAACGAG-3' Reverse 5'-GGTCCCTGCTTGTCTCCATA-3'
ACC2	Forward 5'-CTGGCTGAGGAGATCAAACAG-3' Reverse 5'-TGGGAACTGATCTGGGTGTAG-3'
SCD1	Forward 5'-CCCCTACGACAAGAACATTCA-3' Reverse 5'-CACTGGCAGAGTAGTCGAAGG-3'
ELVOL6	Forward 5'-CGAAGATCAGCCCCAATG-3' Reverse 5'-CAGCGTACAGCGCAGAAA-3'
Glut-1	Forward 5'-TCTCTGTCGGCCTCTTTGTT-3' Reverse 5'-CCAGTTTGGAGAAGCCCATA-3'
Glut-2	Forward 5'-CCCTGGGTACTCTTCACCAA-3' Reverse 5'-GCCAAGTAGGATGTGCCAAT-3'
Glut-4	Forward 5'-GATTCTGCTGCCCTTCTGTC-3' Reverse 5'-CAGCTCAGCTAGTGCGTCAG-3'
G6Pase	Forward 5'-GGATCTACCTTGCTGCTCACTT -3' Reverse 5'-CCAAACAAGAAGATGGTGATGA -3'
PCX	Forward 5'-AGGTCCACATCTGTGATCTCCT-3' Reverse 5'-AAGCAGGTAGGCTATGAGAACG-3'
FBPase	Forward 5'-TCAACTGCTTCATGCTGGAC -3' Reverse 5'-GGGTCAAAGTCCTTGGCATA -3'
PEP-CK	Forward 5'-GGAAGAGGACTTTGAGAAAGCA -3' Reverse 5'-ACATAGGGCGAGTCTGTCAGTT -3'

Results

R-Tf-D-LP4-Mediated Effects on HFD-32-Induced Liver Damage and Functional Markers - Biochemical Analysis at the Steatosis and NASH Stages

The effect of R-Tf-D-LP4 on liver damage and function was revealed by assessing several biochemical parameters. Blood samples from ND-fed, HFD-32-fed and HFD-32-fed, peptide-treated mice were analyzed for the release of liver enzymes, such as alanine aminotransferase (ALT), aspartate aminotransferase (AST) and alkaline phosphatase (ALP). All showed increased levels in blood from HFD-32-fed relative to ND-fed mice. This increase was reduced in HFD-32-fed, peptide-treated mice (Figures S2A-S2C).

Accumulation of fat in the liver is associated with increased cholesterol and triglyceride levels in the blood, as seen in HFD-32-fed mice but was reduced in HFD-32-fed, peptide-treated mice (Figures S2D,S2E). The levels of blood glucose and, phospholipids in the livers of HFD-32-fed mice were increased yet were decreased in the peptide-treated mice (Figures S2F,S2G).

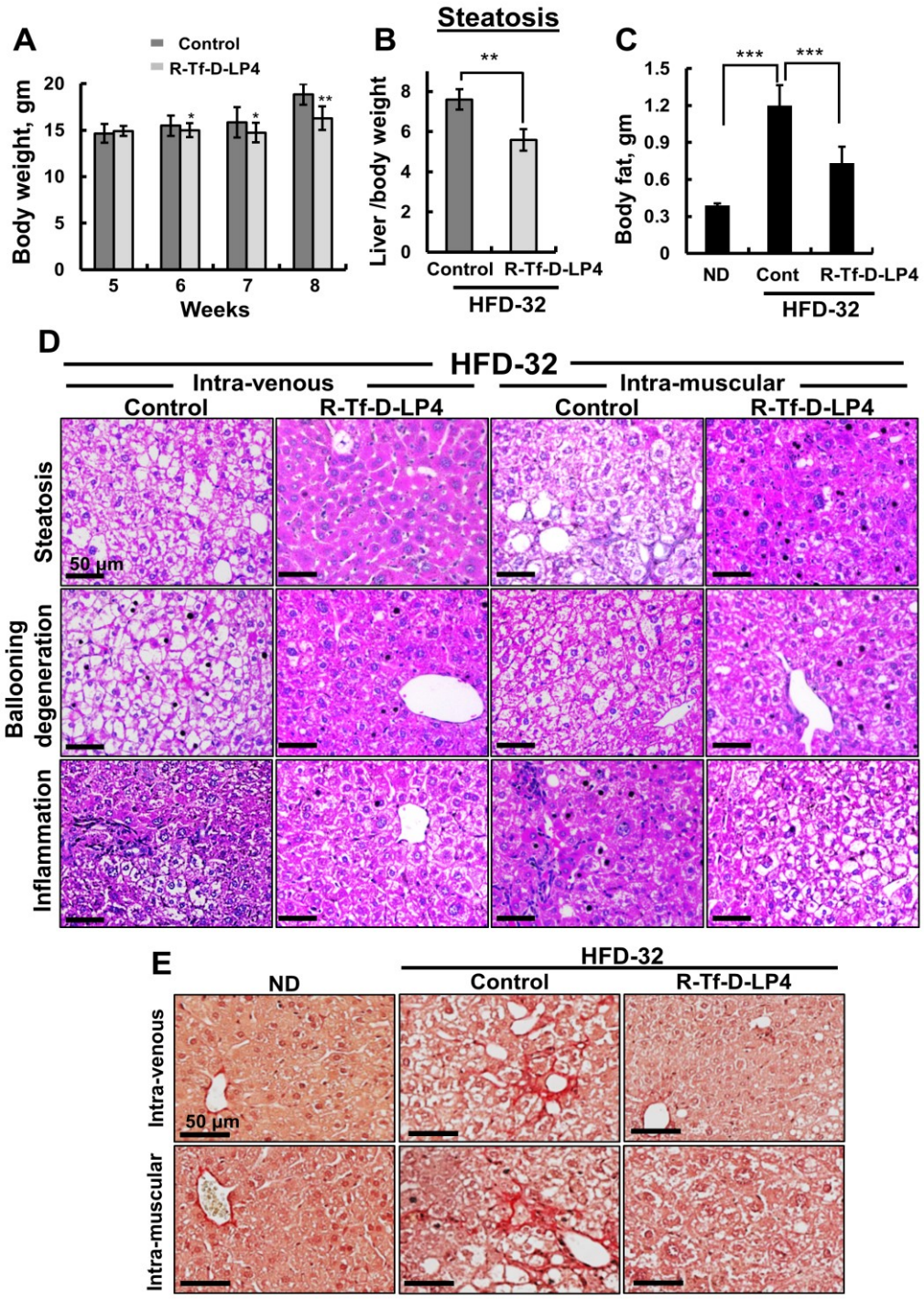

Figure S1. R-Tf-D LP4 Peptide Decreased Liver and Fat Weight and Similarly Inhibited Steatotic Liver Pathology when Administered Intravenously or Intramuscularly to HFD-32-Fed Mice

Mice were ND-fed, HFD-32-fed or HFD-32-fed, and peptide-treated (14 mg/kg, intravenous (i.v.)). Body weight (**A,** 5-8 weeks) and ratios between liver and body weights (**B,** week 8) for HFD-32 without (dark grey) and treated with the peptide (light gray) are shown. The weight of abdominal visceral fat (**C,** week 8) was analyzed for ND-fed and HFD-32 fed without and treated with the peptide. HFD-32-fed were peptide-treated (14 mg/kg) from weeks 6-8 by i.v. or intramuscular (i.m.) injection every two days with 100 µl of 0.8% DMSO in HBSS (control) or R-Tf-D-LP4 (14 mg/kg) in HBSS. Mice were then sacrificed, and liver sections were stained with H&E for assessing ballooning degeneration and inflammation (**D**) or with sirius red (**E**). Results = means ± SEM (n = 5-8 mice), (* $P \leq 0.05$, **$P \leq .01$; ***$P \leq .001$). Images were captured using a light microscope (Leica DM2500).

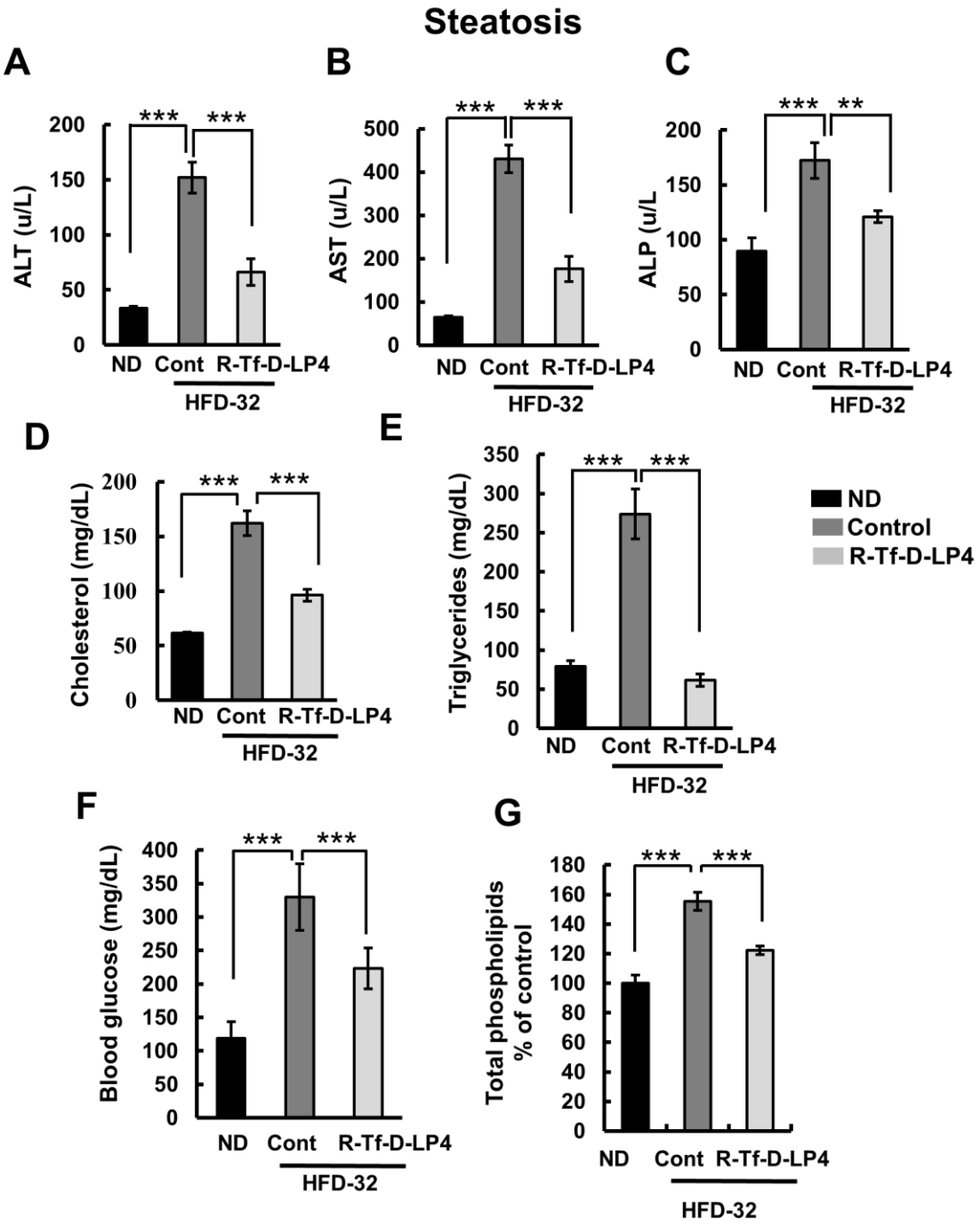

Figure 2S. Serum Biochemical Parameters of HFD-32-Fed Mice Treated or Untreated with the Peptide at Steatosis

Blood was collected from chow-fed, HFD-32-fed and HFD-32-fed, peptide-treated mice (14 mg/kg, i.v.) at the steatosis stage, serum was obtained and analyzed for the liver enzymes ALT (**A**), AST (**B**) and ALP (**C**) **(**presented as units per liter (U/L)**,** and cholesterol (**D**), triglycerides (**E**) and glucose (**F**), all presented as mg/deciliter (mg/dL). The levels of total phospholipids in livers from HFD-32-fed and HFD-32-fed, peptide-treated mice (14 mg/kg), relative to chow-fed mice (**G**). Results = means ± SEM (n = 3–5), (* $P \leq 0.05$, **$P \leq .01$; ***$P \leq .001$).

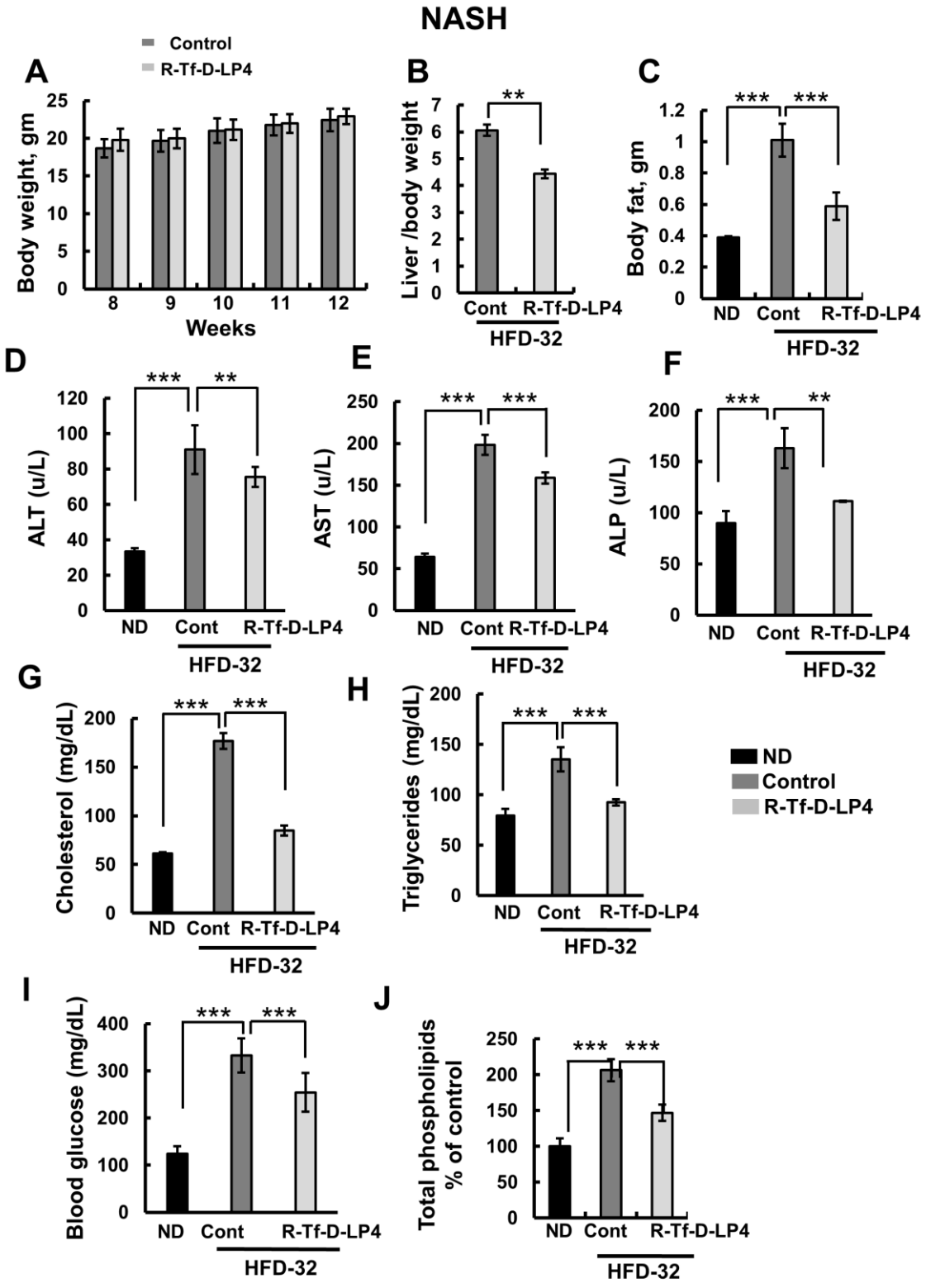

Figure S3. Serum Biochemical Parameters of HFD-32 Mice Treated or Untreated with Peptide at the NASH Stage

Body weight (**A**), the ratio between liver and body weights (**B**), and the weight of abdominal visceral fat (**C**) at NASH were analyzed for chow-fed and HFD-32-fed untreated or peptide-treated (14 mg/kg) mice. Serum from each group (n=10) was analyzed for liver enzymes ALT (**D**), AST (**E**) and ALP (**F**) **(**presented as units per liter (U/L), and cholesterol (**G**), triglycerides (**H**) **(**presented as mg/deciliter, mg/dL) and glucose (**I**). The levels of liver phospholipids were assessed in HFD-32-fed mice untreated or peptide-treated (14 mg/kg), relative to chow-fed mice (**J**). Results = means ± SEM (n = 3–5), (* $P \leq 0.05$, ** $P \leq .01$; *** $P \leq .001$).

Also, as at the steatotic disease stage, blood biochemical analysis of HFD-32-fed mice at the NASH stage showed increased levels of ALT, AST and ALP, relative to ND-fed mice. These levels were decresed in the HFD-32-fed, peptide-treated mice (Figures S3D-S3F). The levels of blood cholesterol, triglycerides and glucose were increased in HFD-32-fed mice b were reduced by the peptide to levels close to those of chow-fed mice (Figures S3G-S3I). The total phospholipid level in HFD-32-fed mice livers was increased 2-fold and significantly decreased upon peptide treatment (Figure S3J).

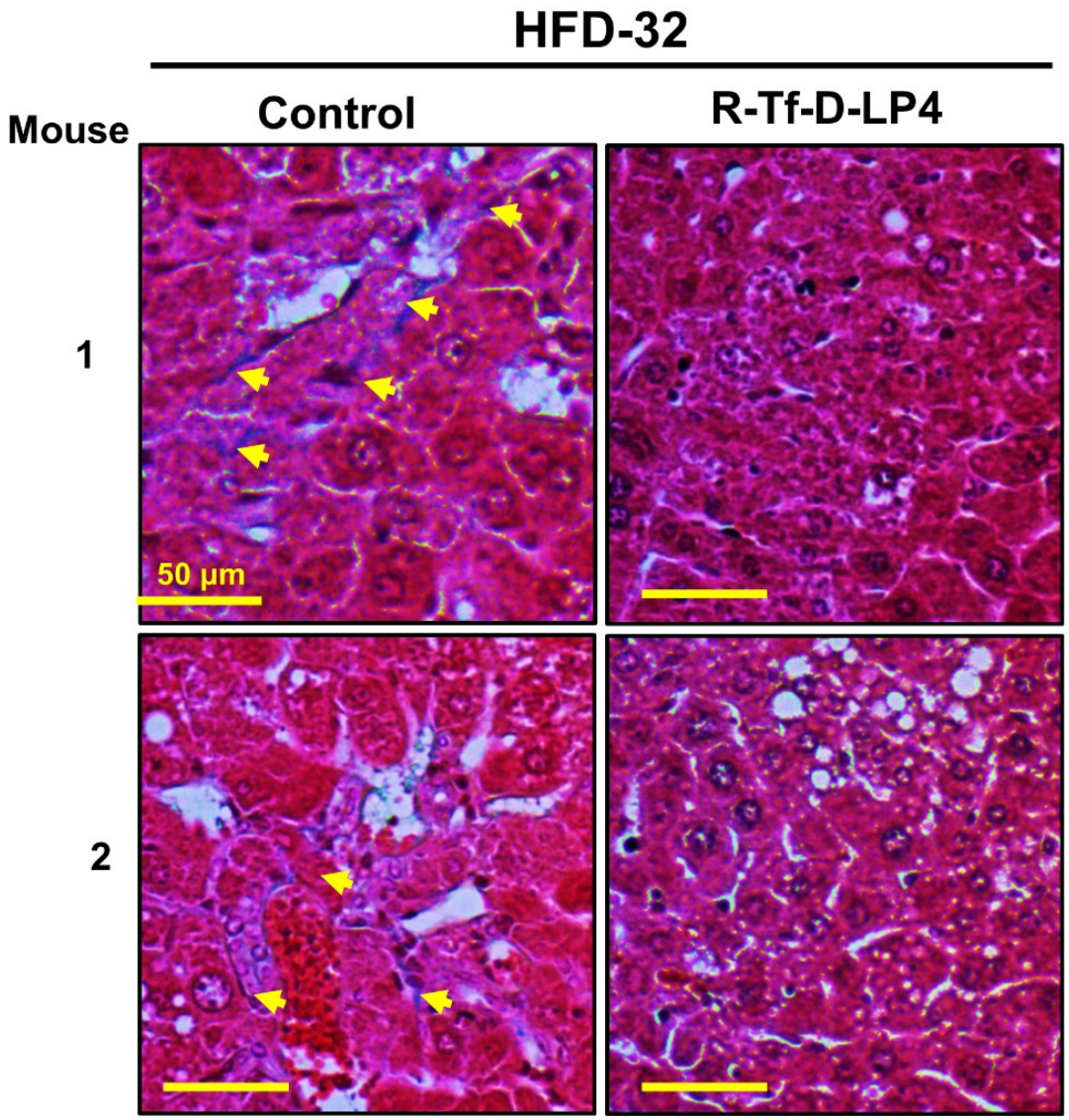

Figure S4. **R-Tf-D-LP4 Peptide Treatment Reduced Fibrosis, as Revealed by Masson's Trichrome Collagen Staining of NASH Mouse Livers**

Representative sections of livers from HFD-32-fed mice or HFD-32-fed mice treated with R-Tf-D-LP4 (14 mg/kg) at NASH were stained with Masson's trichrome stain. Collagen (blue) is depicted by arrows (yellow). Images were captured using a light microscope (Leica DM2500).

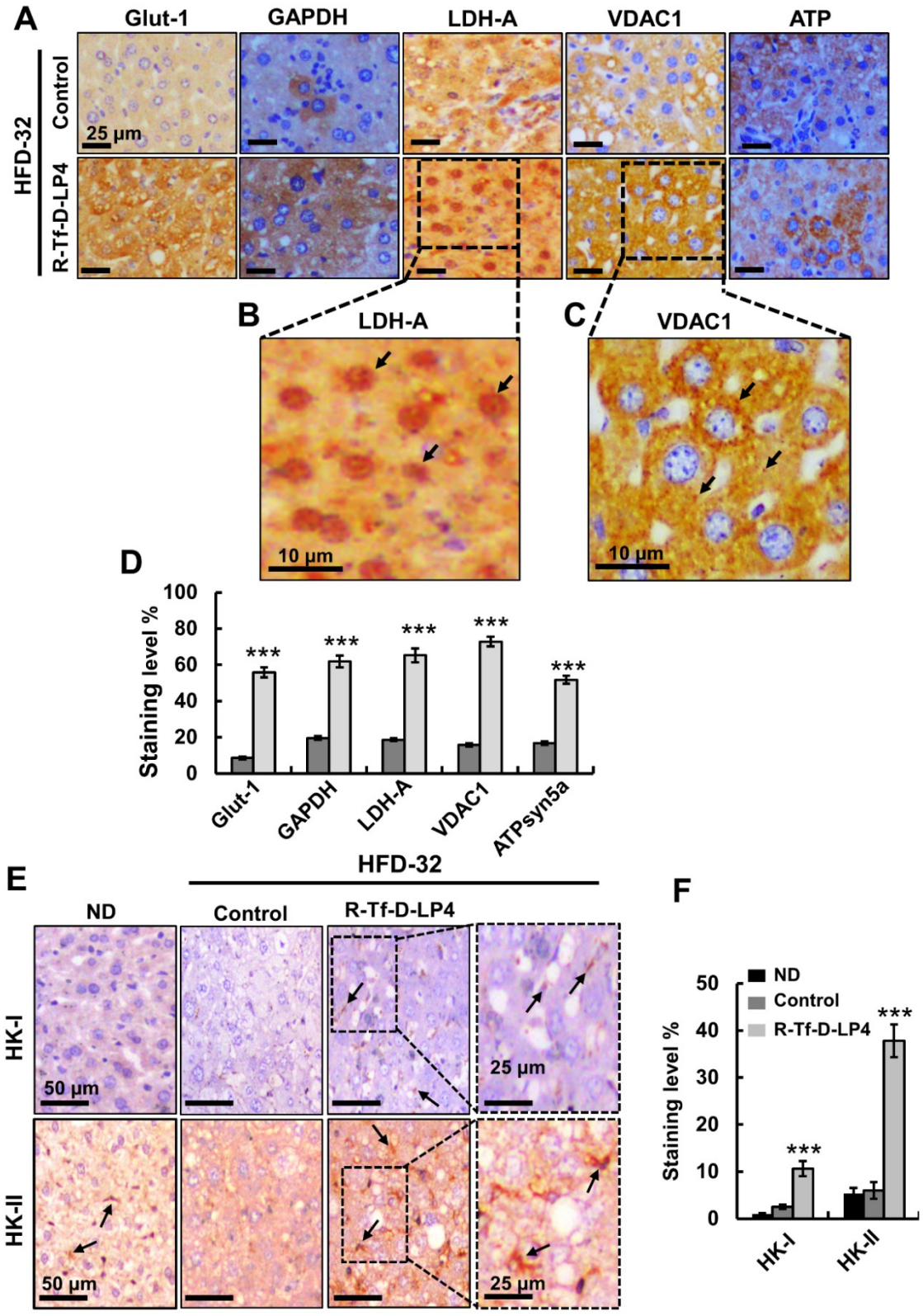

Figure S5. R-Tf-D-LP4 Peptide Treatment of HFD-32-Fed Mice at the NASH Stage Altered the Expression of Metabolism-Related Enzymes

Representative IHC staining (**A**) and quantitative analysis of staining intensity **(D)** of liver sections from ND-fed and HFD-32-fed mice with or without peptide treatment for Glut-1, LDH-A, VDAC1 and ATP synthase 5a. Nuclear localization of LDH-A, some of which is indicated by the black arrows (**B**), and mitochondria-localized VDAC1 (**C**) are shown. IHC for HK-I and HK-II, reveals increased levels in hepatic stellate cells (arrows) (**E**), Quantitative analysis of the IHC images (**F**). Images were captured using a light microscope (Leica DM2500).

R-Tf-D-LP4 Peptide-Mediated Effects on Glycogen Levels and Metabolism

The levels of glycogen and glycogen metabolism-related enzymes in the HFD-32-fed mice without or with peptide treatment at the steatosis and NASH stages were determined (Figure S6). Glycogen levels in livers derived from HFD-32-fed mice and HFD-32-fed, peptide-treated mice were determined following glycogen isolation from frozen liver samples using the calorimetric method based on anthrone in 95% sulphuric acid (Figures S6A,S6B) and by PAS staining of fixed liver sections (Figures S6C,S6D). In both the steatosis and NASH stages, the level of glycogen was decreased in the HFD-32-fed mice, relative to ND-fed mice, and was increased again when the mice were treated with the peptide. qRT-PCR analysis of several enzymes associated with glycogen metabolism showed that glucose-6-phpsphate phosphatase (G6Pase), and phosphoenolpyruvate carboxykinase (PEP-CK), cataplerotic enzyme that functions in gluconeogenesis, and participants in a feeder reaction for carbon from the citric acid cycle to various biosynthetic and oxidative processes[7], were increased in the HFD-32-fed, peptide-treated mice over their levels in ND- or HFD-fed mice (Figures S6E,S6F). On the other hand, the expression levels of pyruvate carboxylase (PCX), and fructose bisphosphatase (FBPase), both involved in gluconeogenesis, were increased in HFD-32-fed mice, while decreased relative to the levels seen in ND-fed mice following peptide treatment of the HFD-fed mice. These results suggest the glycogen is synthesized and also used in de-novo lipid (DLS) syntheses in the HFD-32-fed mice, but both glycogen synthesis and DLS were inhibited in the livers of HFD-fed-peptide, treated mice, where carbohydrates and fat are oxidized.

R-Tf-D-LP4 Peptide-Mediated Effects on Physiological Parameters of HFD-32-Fed Mice in Metabolic Cages

To test the effects of the peptide on the metabolic parameters of HFD-32-fed mice, such mice in metabolic cages were assessed using indirect calorimetry (TSE Systems) (Figure S7). Heat production (energy expenditure, EE) (Figure S7A), respiratory exchange ratio (RER) (Figure S7B), oxygen consumption ratio (OCR) presented as VO_2 (Figure S7C) and carbon dioxide production (VCO_2)(CDP) (Figure S7D) were evaluated.Rates of EE (kcal/h/kg) were increased by 10-20% in HFD-32-fed, peptide-treated mice, as compared to untreated HFD-32 mice (Figure S7A).

An RER value of 0.8 reflects normal diet, while values of 1.0 and below 0.7 indicate that carbohydrates or fat, respectively, are the primary energy source. As expected, for HFD-32-fed mice, the RER was about 0.7 and decreased to about 0.6 in peptide-treated mice in both dark and light cycles (Figure S7C), indicating a high use of fat. OCR and CDP levels were also increased in HFD-32-fed, peptide-treated mice, relative to their values in HFD-32-fed mice (Figures S7C,S7D,), in accord with respiratory-based metabolism. Experiments using metabolic cages showed that peptide treatment had no effect on locomotor activity (Figure S7E), but led to a slight increase in

food intake (Figure S8A,B) and an increase in water consumption (Figure S8C). The results suggest that peptide treatment of HFD-32-fed mice led to higher use of fat while producing more heat.

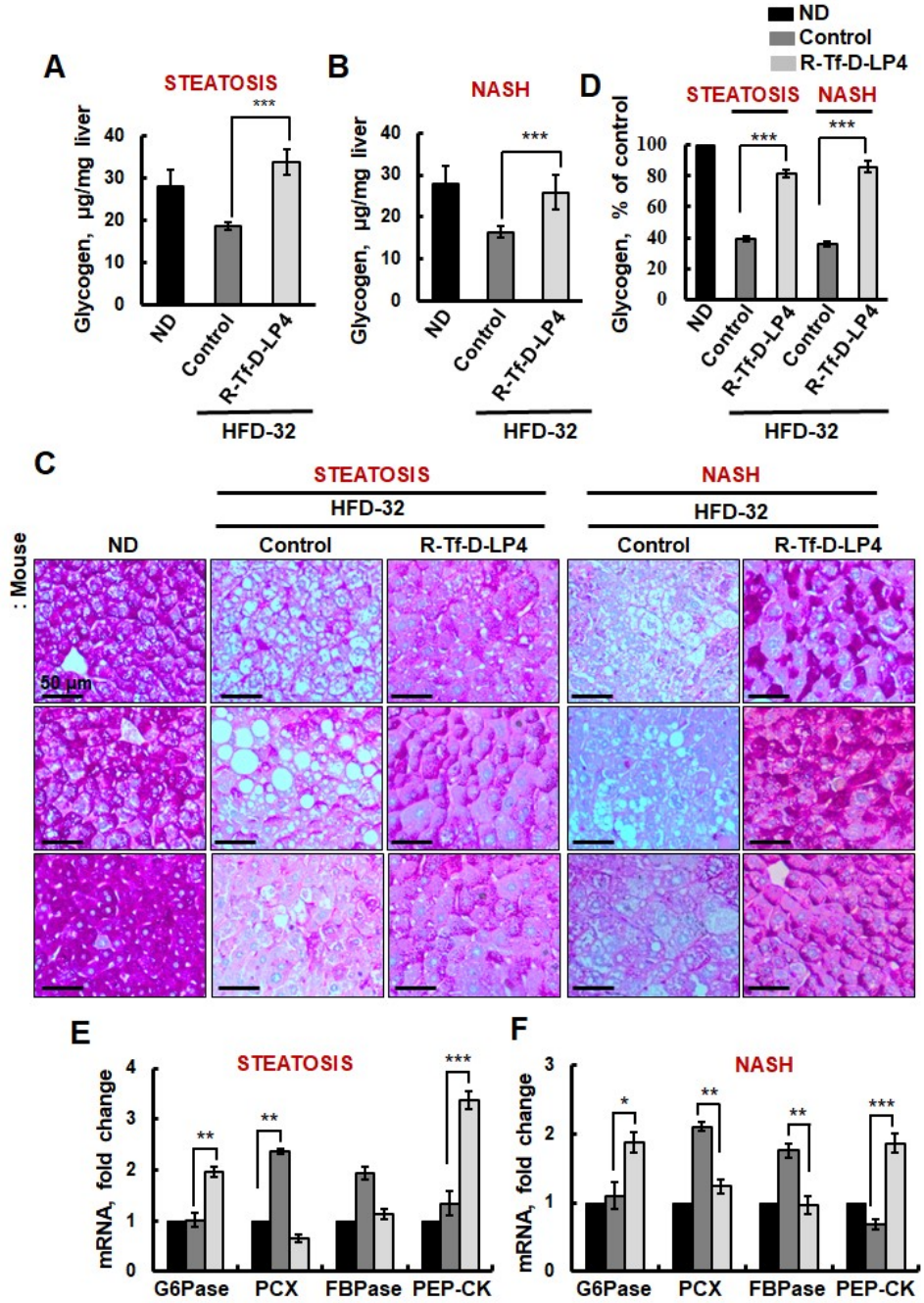

Figure S6. R-Tf-D-LP4 Peptide-Treatment of HFD-32 Mice Restores Glycogen Levels and Altered Gluconeogenesis

Glycogen was isolated from frozen livers derived from chow-fed, HFD-32-fed and HFD-32-fed, peptide-treated mice at the steatosis (**A**) or NASH (**B**) stage. Glycogen levels were determined as described in the Supplementary Information section. **C,D**. PAS staining of fixed liver sections obtained from ND-fed mice, HFD-32-fed mice untreated or treated with R-Tf-D-LP4 peptide in the steatosis and NASH stages (**C**); quantification of the PAS-stained sections after scanning with a panoramic scanner (panoramic MIDI II, 3DHISTH) and using HistoQuant software (Quant Center 2.0 software, 3DHISTH) (**D**). **E,F.** qRT-PCR analysis of mRNA levels of enzymes associated with glycogen metabolism, glucose-6-phosphate phosphatase (G6Pase), phosphoenolpyruvate carboxykinase (PEP-CK), pyruvate carboxylase (PCX), and fructose bisphosphatase (FBPase) at the steatosis (**E**) and NASH (**F**) stages in chow-fed mice (black bars), HFD-32-fed mice untreated (dark gray bars) or treated with R-Tf-D-LP4 peptide (light gray bars). Results = means ± SEM (n = 3–5) (* $P \leq 0.05$, ** $P \leq .01$; *** $P \leq .001$).

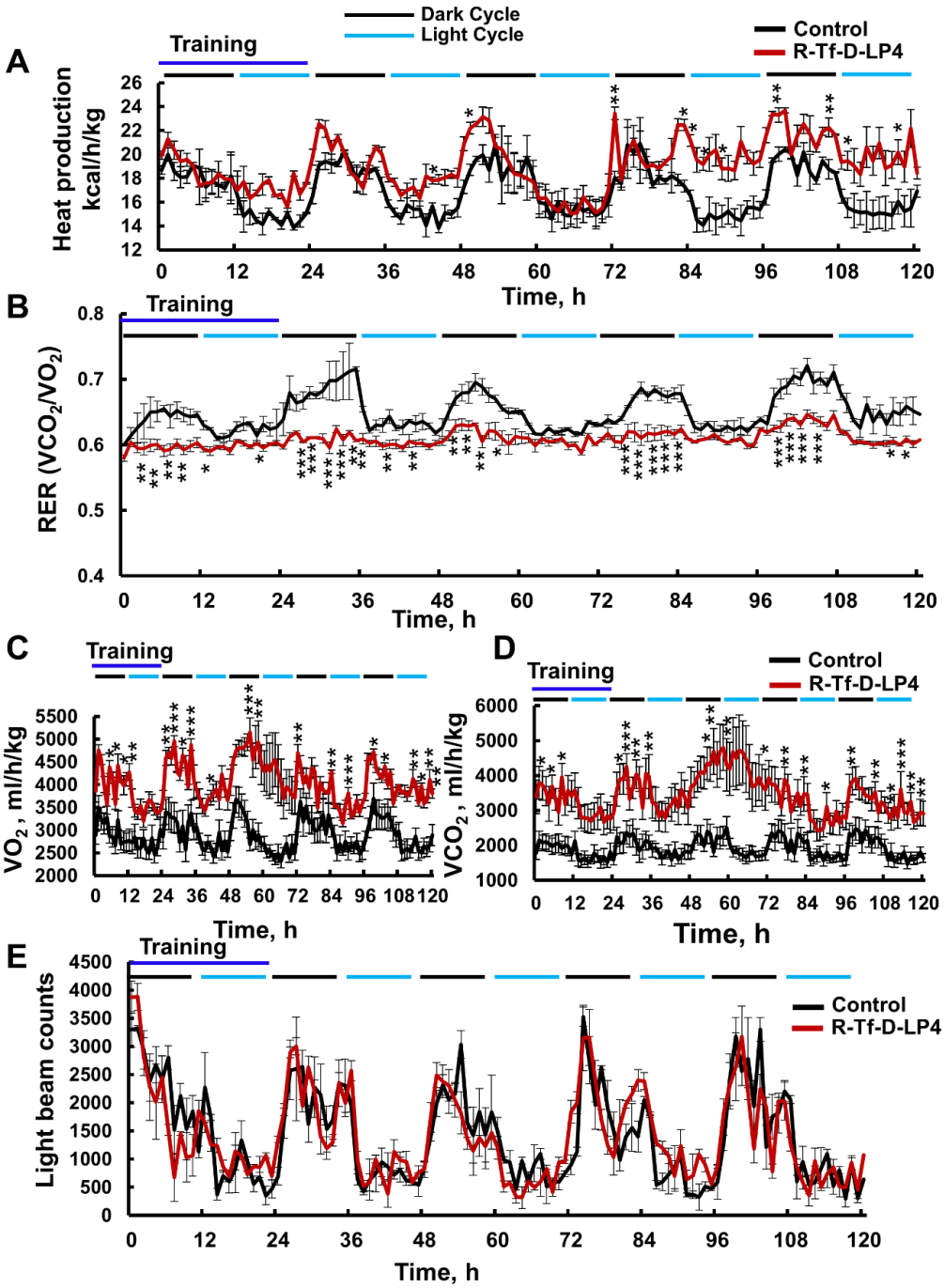

Figure S7. Metabolic Parameters and Energy Expenditure of HFD-32 Mice at the Steatosis Stage With or without Peptide Treatment

Mice at the steatosis state fed a HFD-32 diet and untreated or treated with R-Tf-D-LP4 peptide (14 mg/kg), were individually housed in PhenoMaster metabolic chambers (LabMaster system; TSE-systems), as described in the Methods section. The mice were acclimatized for 24 h prior to data recording. Automated monitoring of metabolic parameters and behaviour was continuously performed using a CLAMS (Comprehensive Lab Animal Monitoring System; Columbus Instruments) open-circuit indirect calorimetry system. Data were collected over 48 h (i.e., on the last 2 days of the experiment). **A**. Energy expenditure normalized to lean body weight ($kcal.h^{-1}.kg^{-1}$).**B**. Respiratory exchange rate (RER; VCO_2/VO_2). **C**. Whole body oxygen consumption rate (VO_2). **D**. Whole-body carbon dioxide expiration rate (VCO_2). **E**. Locomotor activity of the mice was measured continuously over the 5 days, using a CLAMS, as determined by light beam counts (sum of horizontal and vertical counts). Measurements were recorded on a cycle of dark and light (black and blue lines, respectively). Results = means ± SEM (n = 3–4) (* $P \leq 0.05$, ** $P \leq .01$; *** $P \leq .001$).

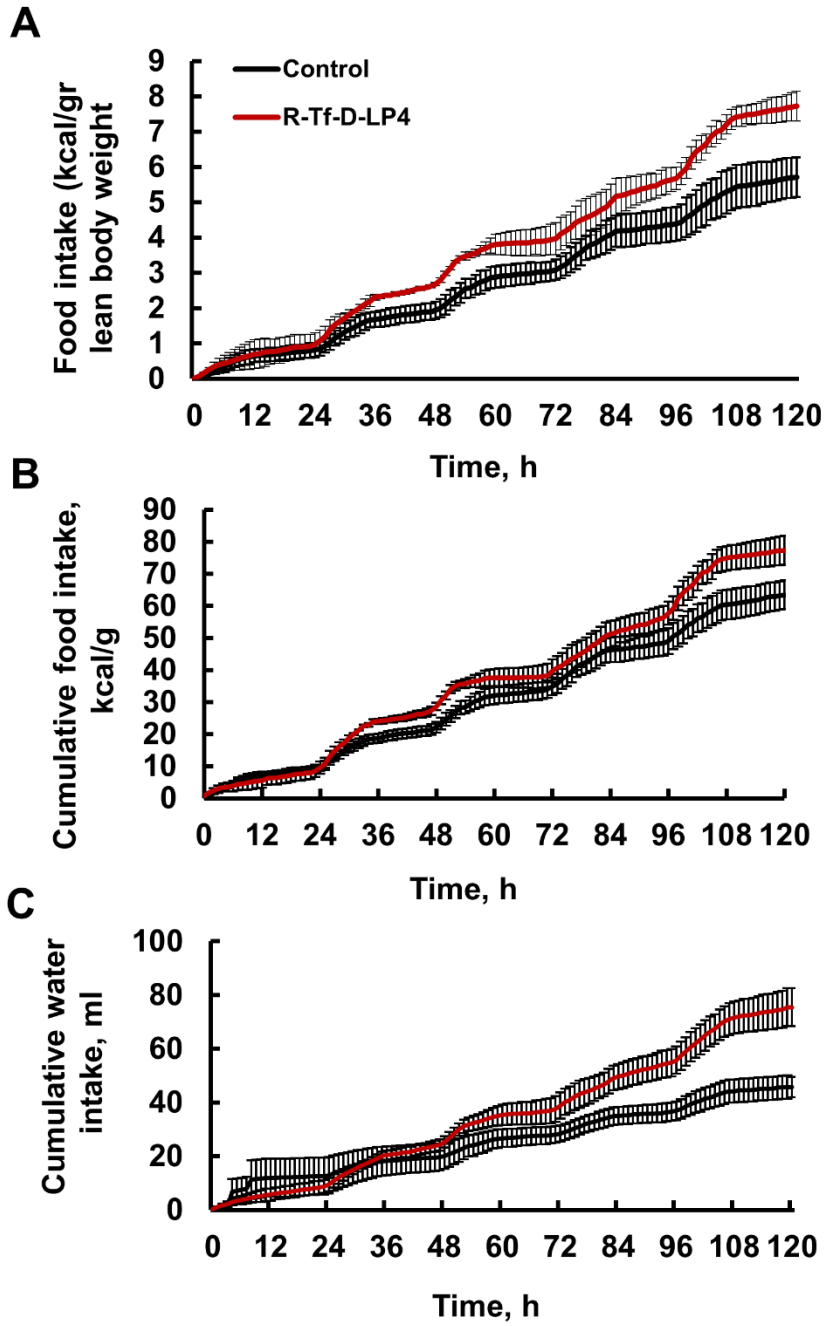

Figure S8. Food and Water Consumption By HFD-32-Fed Mice Treated or Untreated with Peptide at the Steatosis Stage – Metabolic Cages

(**A**) Food intake relative to lean body weight for HFD-32-fed mice untreated (black line) or peptide-treated (14 mg/kg) (red line). (**B**) Cumulative food intake presented in kcal/g. (**C**) Cumulative water consumption by HFD-32-fed mice (black line) or HFD-32-fed, peptide-treated mice (14 mg/kg) (red line).

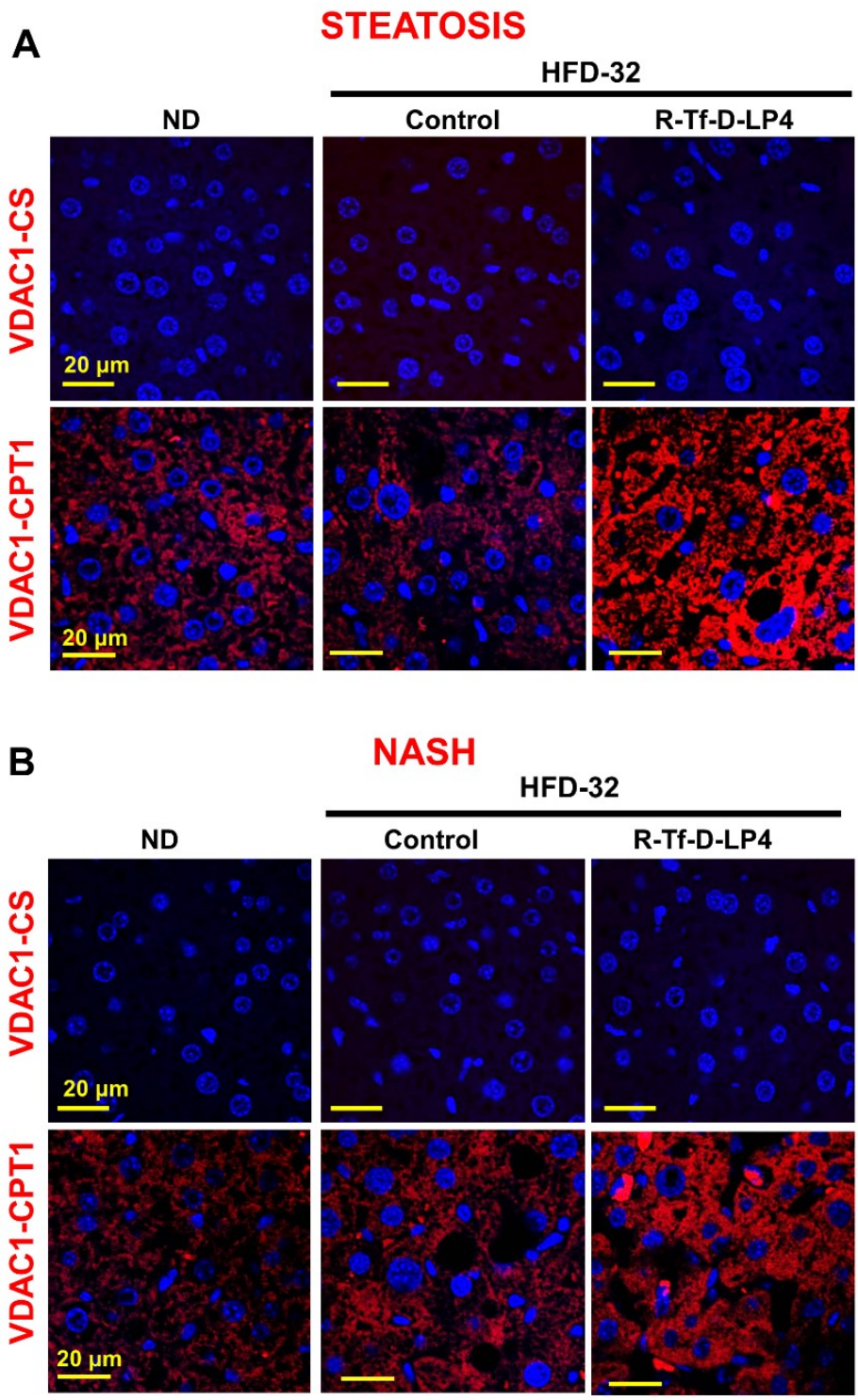

Figure S9. Peptide-Treated Mice Increase the Interaction of VDAC1 with CPT1a but not of VDAC1 and Citrate Synthase, as Revealed using a Proximity Ligation Assay

Liver sections from HFD-32-fed mice at the steatosis (**A**) or NASH (**B**) stage, untreated or treated with R-Tf-D-LP4 peptide (14 mg/kg) were subjected to *in situ* PLA, as described in the Method section. *In situ* PLA was carried out for VDAC1/CPT1 and VDAC1/citrate synthase (CS) and counterstained with DAPI. Images were captured using a confocal microscope (Olympus IX81).

References

1 Prezma, T, Shteinfer, A, Admoni, L, Raviv, Z, Sela, I, Levi, I*, et al.* (2013). VDAC1-based peptides: novel pro-apoptotic agents and potential therapeutics for B-cell chronic lymphocytic leukemia. *Cell Death Dis* **4**: e809.

2 Fujii, M, Shibazaki, Y, Wakamatsu, K, Honda, Y, Kawauchi, Y, Suzuki, K*, et al.* (2013). A murine model for non-alcoholic steatohepatitis showing evidence of association between diabetes and hepatocellular carcinoma. *Med Mol Morphol* **46**: 141-152.

3 Zhang, Y, Xu, N, Xu, J, Kong, B, Copple, B, Guo, GL*, et al.* (2014). E2F1 is a novel fibrogenic gene that regulates cholestatic liver fibrosis through the Egr-1/SHP/EID1 network. *Hepatology* **60**: 919-930.

4 Wang, P-X, Zhang, X-J, Luo, P, Jiang, X, Zhang, P, Guo, J*, et al.* (2016). Hepatocyte TRAF3 promotes liver steatosis and systemic insulin resistance through targeting TAK1-dependent signalling. *Nature Communications* **7**: 10592.

5 Gustafsdottir, SM, Schallmeiner, E, Fredriksson, S, Gullberg, M, Söderberg, O, Jarvius, M*, et al.* (2005). Proximity ligation assays for sensitive and specific protein analyses. *Analytical biochemistry* **345**: 2-9.

6 Liang, W, Menke, AL, Driessen, A, Koek, GH, Lindeman, JH, Stoop, R*, et al.* (2014). Establishment of a general NAFLD scoring system for rodent models and comparison to human liver pathology. *PloS one* **9**: e115922-e115922.

7 Yang, J, Kalhan, SC, and Hanson, RW (2009). What is the metabolic role of phosphoenolpyruvate carboxykinase? *Journal of Biological Chemistry* **284**: 27025-27029.